CHARACTERIZATION OF WRINKLING AND DE-WRINKLING BEHAVIOUR OF WOVEN FABRICS USING A MULTI-STEP BIAXIAL BIAS EXTENSION TEST

A. Rashidi, A.S. Milani*

Composites Research Network-Okanagan Laboratory, School of Engineering
University of British Columbia, Kelowna, Canada
*abbas.milani@ubc.ca

Keywords: woven fabric composites, wrinkling, de-wrinkling, multi-step biaxial bias extension test, tow slippage

Abstract
Wrinkling is one of the most common defects occurring during forming process of composite materials with complex mould shapes. It is of interest to designers to predict the minimum magnitude of forces required to mitigate wrinkles in useful regions of the part, through appropriate boundary conditions imposed by the blank holders. Toward this goal, in this article a new characterization technique, namely a multi-step biaxial bias extension (MBBE) test, has been proposed to determine the amount of required transverse de-wrinkling force, in order to flatten the wrinkles of different sizes while shearing a typical polypropylene/glass plain weave fabric. Using a handheld 3D scanner and image processing, variables such as local shear angles and the onset of wrinkling as well as the geometrical properties of the defect (e.g., wrinkle height and area) were characterized. The underlying deformation mechanism and the wrinkling/de-wrinkling force responses of the fabric were investigated and correlated to the aforementioned variables, resulting into some potential practical design considerations for future 3D forming applications. Furthermore, the influence of yarn contact forces and tow slippage was noted to be considerable in devising de-wrinkling strategies.

1. Introduction

Among various types of composites, woven fiber-reinforced polymers have become a leading genre in industries such as automotive, defense, and aerospace, mainly due to their high impact resistance capacity along with conformability to complex 3D contours [1]. Yet, there exist ongoing challenges as to properly form woven fabric reinforcements without manufacturing faults and defects, especially when it comes to draping over double-curved geometries which necessitate large in-plane shear deformations [2]. Depending on the geometry of a final part, as well as the given fabric characteristics and manufacturing parameters, defects during the double-curved shape forming can be problematic and not fully controllable. Wrinkling is one of the most frequent defects seen during forming processes of woven composites, leading to unexpected interruptions during manufacturing, or causing a notable reduction in mechanical properties of the final product [3]. Studies have been carried out to characterize the shear response of fabric reinforcements as it is the primary forming mechanism behind wrinkling during the draping of double curved geometries [4, 5]. These studies have primarily employed the picture frame (PF) and/or bias-extension (BE) tests in order to understand the woven material's formability, and eventually to develop accurate constitutive models of fabrics for forming simulation and wrinkle predictions. For instance, Harrison et al. [6] devised a new characterization approach, namely a biaxial bias extension (BBE) test, in which constant transverse forces were applied to the sample while performing a conventional uniaxial bias extension (BE) test. It was observed that increasing membrane tensions effectively delays the onset of wrinkling. Wrinkling is generally assumed to take place when the shear deformation goes beyond a certain limit. For many years, the so-called 'locking angle' was considered to be a key local characteristic (limiting value) in identifying the

Excerpt from ISBN 978-3-00-053387-7

onset of wrinkles; however, recent numerical models revealed that wrinkling can arise from a global mechanical problem depending on the yarns rigidity and strains applied to the fabric [2], hence more comprehensive studies began to take place in order to better characterize this phenomenon and ultimately develop most cost effective strategies to mitigate wrinkles during forming process of different types of fabrics.

The present experimental work, as the first step of a larger research program at the Composites Research Network (CRN) aims to extend our understanding of mechanisms behind formation of wrinkles in woven fabrics and consequently seeking for new strategies to vanish them via appropriate de-wrinkling forces. The manuscript has been structured as follows. Section 2 begins with a description of the test material and a new characterization setup (MBBE) used in the characterization experiments. In Section 3, the deformation mechanisms occurring during the wrinkling/de-wrinkling tests are discussed. Results are presented in Section 4 and some considerations in characterizing the wrinkling defect in the context of fiber slippage and yarns tension are outlined. Conclusions are included in Section 5.

2. Methodology

2.1. Material

The material (Figure 1) selected for the experiments was a typical comingled polypropylene/glass plain weave composed of 40% (by weight) Polypropylene (PP) thermoplastic fibers and 60% E-glass reinforcement fibers.

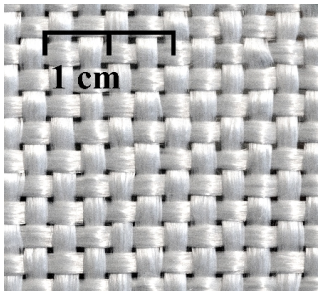

Figure 1. Balanced PP/glass plain weave fabric.

2.2. Test setup

2.2.1. Custom biaxial fixture

Experiments were conducted using the newly developed custom biaxial fixture (Figure 2a). The device consists of four aluminum bars connected using tubular bearings while positioned orthogonally. Four servomotors are installed perpendicular to the arms along with their corresponding jaws in order to apply global axial displacement to the test material (Figure 2b). The biaxial motors are equipped with load-cells and linear variable differential transformers (LVDT) to monitor forces and displacements over time. Fixture arms can be moved apart by a test speed of 4mm/min in all four directions. The grips holding the material include vertical needles, between which the test sample is held with no slippage. The loading width was chosen as 70 mm for both transverse and longitudinal clamps. As shown in Figure 2b, the specimens were cut with an aspect ratio of 3.85 where L=270 mm and W=70 mm are the length and width of the sample, respectively. A white base plate was placed underneath the sample to facilitate the 3D scanning process and prevent scanning undesirable objects around the sample. Three replications were performed for all tests.

Excerpt from ISBN 978-3-00-053387-7

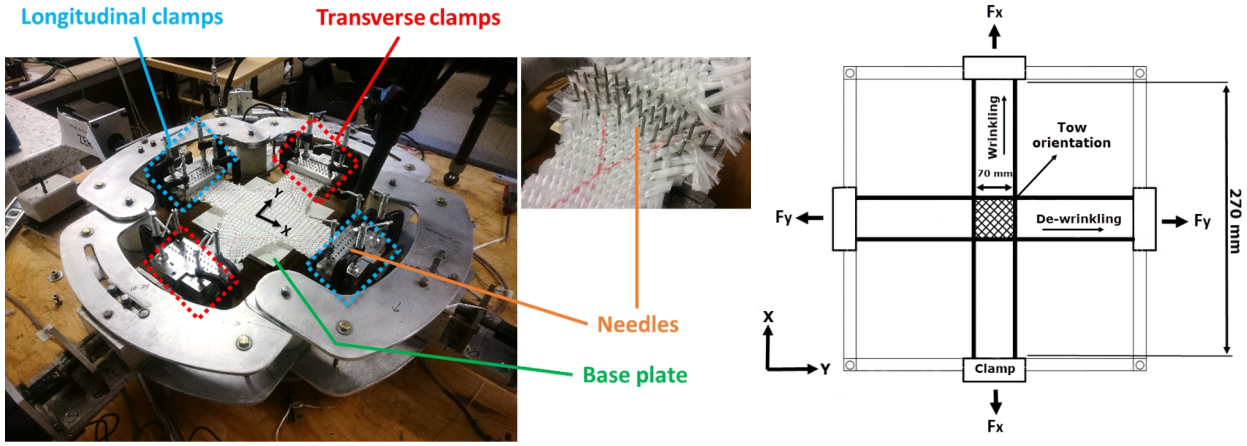

(a) (b)

Figure 2. (a) The custom biaxial fixture used for the multi-step biaxial bias extension tests; (b) Four servomotors mounted on the arms shear the biaxial fabric specimen in the bias (originally mounted at ±45°) direction.

2.2.2. Multi-step biaxial bias extension (MBBE) test method

Figure 3 illustrates the proposed multi-step biaxial bias extension test procedure. Namely, a wrinkle via the longitudinal (x-direction) loading is generated while the transverse edges of the cross-shape fabric are free (as if performing a conventional uniaxial bias extension test where the wrinkling may initiate in early stages of shearing far before the locking, especially for reinforcements with higher yarn bending stiffness [2] which can be experimentally mimicked e.g. by partial pre-consolidation of the fabric). After generating the first (low-level) wrinkle, the motors in the longitudinal direction (x-direction) are stopped and the transverse edges of the fabric are clamped to the jaws on the y-direction. Subsequently, the transverse motors are turned on and the previously formed wrinkle is smoothed-out (de-wrinkles) by extending the fabric in the transverse direction (Stage A in the diagram of Figure 3). Once the wrinkle is flattened (Figure 2) and de-wrinkling force is recorded, the transverse edges can be retrieved to the initial stage by moving the transverse motors to the initial zero-displacement position, leading into formation of the original wrinkle (Stage B in the diagram). Afterwards, the transverse edges are unclamped and the next-level wrinkle can be generated along the longitudinal direction. The same procedure is repeated for the third wrinkle and the force-displacement curves for forming the three wrinkles and their corresponding de-wrinkling process are obtained. It is to note that in this method, each subsequent wrinkle should automatically result in a higher state of defected region at a higher shear angle.

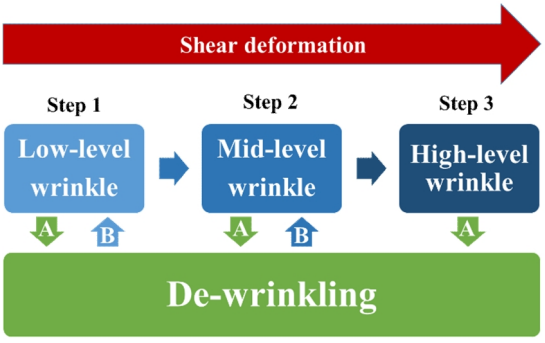

Figure 3. Test sequence in the MBBE experiment.

Excerpt from ISBN 978-3-00-053387-7

2.2.3. Measurement setup for shear angle and geometrical properties of wrinkles

Tests were recorded using two digital cameras mounted on the top of the setup (Figure 4a) and the sample shear deformation in the effective region was quantified using image processing (for each test repeat, images were taken every five seconds). In order to measure the geometrical properties of the wrinkles, a portable Creaform Viuscan 3D scanner (Figure 4b) was used to reconstruct the surface profile of the defected sample, with a precision of 0.5 mm. The scan mesh was generated using the DesignX software.

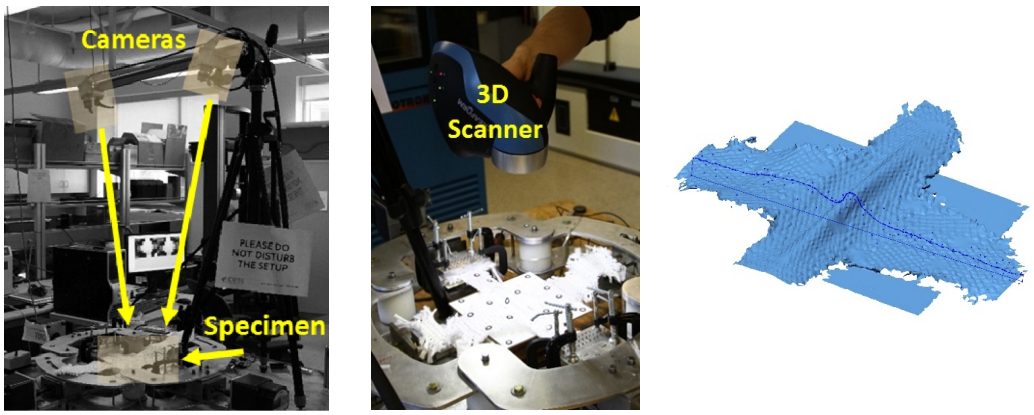

(a) (b) (c)

Figure 4. (a) The test fixture equipped with optical measurement system; sample positioning was monitored via DIC cameras; (b) Scanning the sample surface profile using a portable 3D scanner after formation of each wrinkle; (c) Scanned profile of a wrinkled sample.

4. Results and Discussion

4.1. Observed deformation mechanisms

For the uniaxial and biaxial bias extension tests, the shear distribution is not uniform throughout the sample (Figure 5): regions A, B and C indicate the areas that, under an ideal trellising shear kinematics, possess shear angles of α, α /2 and 0, respectively during a standard BE test step. Such angle distribution is theoretically valid if the fabric is assumed to be a pin-jointed net (PJN) without inter-ply slippage [7]. A rectangular region of interest with uniform shear strain was defined in the middle section of the MBBE samples, whose length and width were variable for each wrinkle level. In particular, the aforementioned theoretical angle distribution is approximately met, as long as the aspect ratio of the specimen is greater than two [8]. During the transverse loading stage (i.e., de-wrinkling) two smaller BE-like regions were formed on either side of region A, as shown in Figure 5 (with unequal W_1 and W_2 widths). Note that during the latter loading step, the sample in the x-direction is clamped while the x-motors are off, and hence the x-movement of region A is restricted.

4.2. Analysis of the wrinkling force

Figure 6 shows the generated wrinkles according to the test procedure in Figure3, along with their corresponding force-shear angle response during each step of the test. The final shear angle at each step was measured from the photos taken upon the formation of wrinkle and stopping the test. The reported angles in Figure 6a were at the corner of the middle region where the fabric was flat, and averaged over three test replicates. With an aspect ratio of greater than two, the existence of yarns with free ends in the middle region of the BE specimens allows having wrinkles with shear angles less than that of seen in the typical picture frame tests (typically occurring around 55° for a similar fabric [9]), hence mimicking a boundary condition somewhat closer to the practical deformations during the thermo-forming processes. Two potential hypotheses for early wrinkling (the onset at 32° shear as seen in Figure 6a) may be offered, both relying on the fact that during the BE test the inward y-axis resultant forces in the middle of the specimen (Zone A in Figure 5) help the sample to buckle with a

Excerpt from ISBN 978-3-00-053387-7

minimum resistance. First, the formation of a smaller loading width (during the x-direction BE loading) compared to the width of sample at the grips may intensify stresses in the mid region. Second, handling errors during mounting of the specimen, or even a slight misalignment inside the fabric, can be spurring the fabric to wrinkle via premature mismatch between the local deformation of the fabric and that of the global fixture. The latter may be further explained by the minimum potential energy principal [9] and the contribution of different mechanisms to deformation energy; namely, the required energy for slippage occurrence (e.g., for yarns with one free end in the mid region) is relatively larger than that for wrinkling, hence causing the latter to occur earlier with no slippage involved (see Figure 6). In summary, depending on the geometry of the mould, some wrinkles at small shear angles can form, especially when sufficient in-plane tensile forces are not available within the fabric [10]. The study [2] has shown that these premature wrinkles are even more severe for samples with yarns of higher bending stiffness.

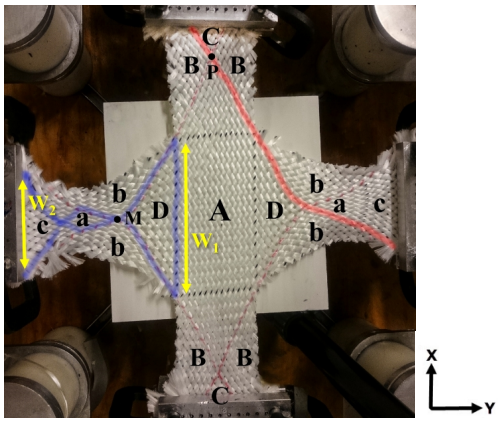

Figure 5. A de-wrinkled state of the fabric with distinguished deformation regions; The red line shows a full fiber path connecting the longitudinal and transverse clamps. Purpole paths indicate different transverse regions developed after de-wrinkling; in fact two transverse BE-like tests on either side of the region A were formed during the de-wrinkling stage; Note that region A would be the main region of interest in forming the final product.

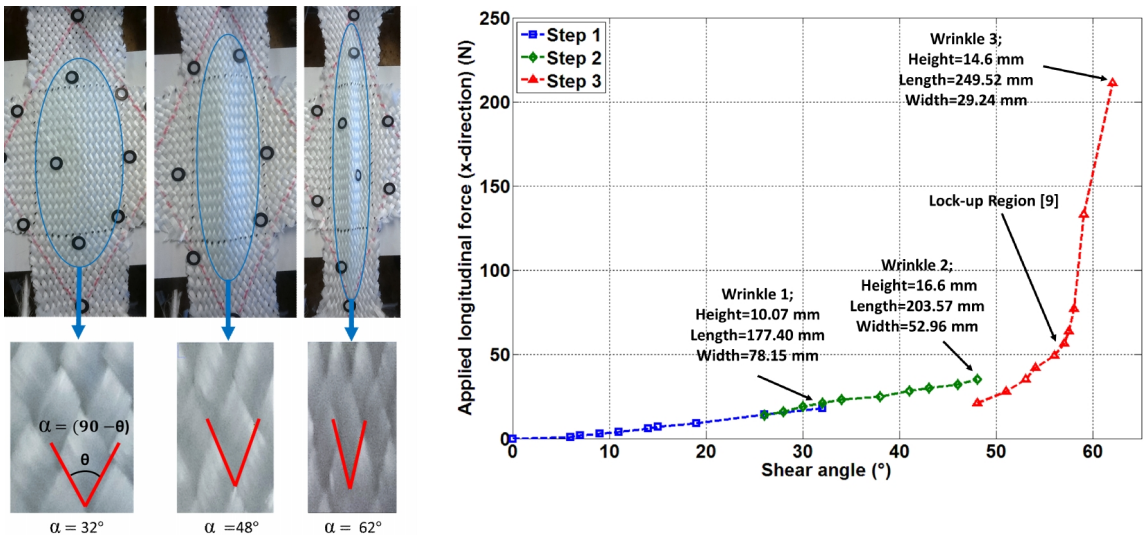

(a) (b)

Figure 6. (a) Generated wrinkles in the x-direction along with their corresponding shear angles; (b) Applied force in the longitudinal direction versus shear angle for the three wrinkle levels. After smoothing out each wrinkle using transverse force and retrieving the transverse strip back to the initial wrinkle, a slight drop was observed in the force (e.g., to stress relaxation) as seen in Figure 6.

Excerpt from ISBN 978-3-00-053387-7

4.3. Analysis of the de-wrinkling force

The results of the de-wrinkling of the medium level wrinkle (i.e., wrinkle 2) is shown in Figure 7 as a sample where the net y-axis force is plotted against the net displacement of the transverse clamps. For all the three defect levels, the de-wrinkling force exhibited a non-linear behavior. As the wrinkles were smoothed out, two bias extension tests with irregular geometries were formed on either side of the wrinkle in the rectangular region of interest (Figure 5). The latter irregularity is due to the difference between the given clamping width in the left side (W_2) and the ensuing width of the right side (W_1) which increases along the x-axis during each test step. As the de-wrinkling process began, the transverse sample strips started to shear, assisting to flatten the associated wrinkle in region A. Similar to the conventional bias extension test, there existed regions containing approximately α, α /2 and 0 shear angles in each smaller BE test in the transverse direction. These regions are marked as a, b, and c, respectively, in Figure 5. Video analysis of the de-wrinkling course indicated that the shear rate throughout the sample is not uniform; especially once the shear angle in the middle region of the transverse strips reached the locking angle due the transverse loading, the entire transverse strips acted similar to a rigid body and extended out the wrinkle with a high rate until it is totally vanished. Hypothetically, if the upper un-deformed triangle (zone D in Figure 5) nearby wrinkle was fixed (clamped), the fabric would start buckling again in the middle zone due to the lock-up. Furthermore, the small sample sizes of the two transverse BE tests resulted in a higher shearing rate (compared to the x-axis BE test stage) and consequently, the fabric underwent higher shear deformation in the middle zone (e.g., 53° shear in zone 'a' during the transverse BE test compared to 48° shear in zone A for the mid-level wrinkle in the longitudinal BE test). It is worth mentioning that after the complete de-wrinkling, the shear angle of zone A was moderately reduced (for example, it reduced from 48 (Figure 6a) to 40° (Figure 7b) in the case of mid-level wrinkle test; suggesting that some level de-shearing is taking place during the course of de-wrinkling in the current test procedure.

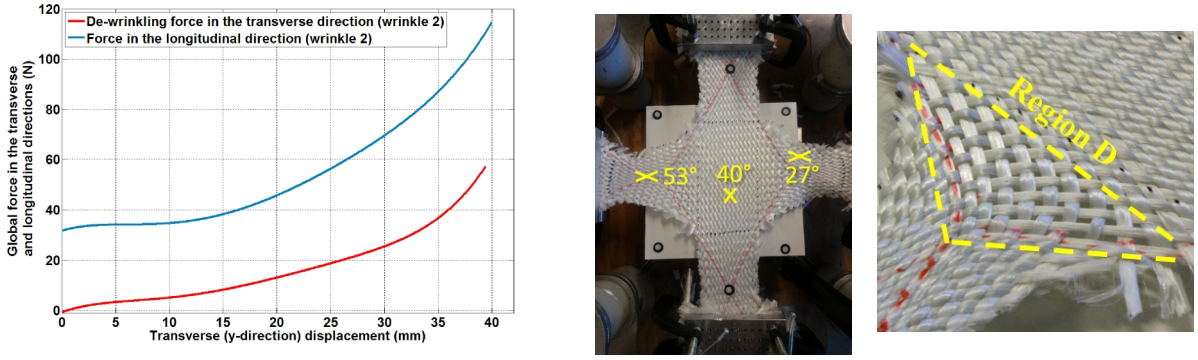

(a) (b) (c)

Figure 7. (a) The de-wrinkling force versus displacement in the transverse direction in step 2 of the MBBE test; the 'reaction' motor force in the longitudinal (x-direction) during the transverse loading has also been added for comparison purposes (note the two curves are almost parallel). (b) The ensuing shear angle at selected regions at the end of the mid-level de-wrinkling test; (c) A zoomed-in area of the slippage (region D in Figure 5).

In addition to the de-wrinkling force in the transverse direction, the reaction force in the longitudinal direction was measured as shown in Figure 7a. Although during the de-wrinkling the fabric was locked along the longitudinal direction (u_x=0), an increase in the force was observed in that direction as the de-wrinkling proceeded in y-direction (with the two force curves rising almost parallel to each other). The increase in the x-axis 'reaction' force is due to the shear residual effect in the x-direction as well as the presence of some full yarn paths directly connecting the longitudinal and transverse clamps (shown in red in Figure 5). More specifically, during the course of the de-wrinkling, as the transverse bias extension test progresses, it attempts to de-shear the x-axis BE test region; however, this is not readily feasible since the x-axis clamps are fixed. Thus there becomes a reaction force in the x-motors;

Excerpt from ISBN 978-3-00-053387-7

i.e., shear coupling between bias extension tests in x and y-directions. Video analysis revealed that point M (shown in Figure 5) in the theoretically un-deformed triangle (region D) remains fixed while de-wrinkling takes place; this would suggest that the tip of the wrinkle (point P) does not move towards the center of region A during the de-wrinkling. In addition, the shear angle at the corner of region A remains constant, implying that no shear deformation occurs in that area during the de-wrinkling. As a result, it can be concluded that tensile forces would develop in the longitudinal direction. A main source of initiation of these tensile forces would be the two triangles nearby the wrinkle (zones D). As the transverse bias extension proceeds, these triangles begin to move in y-direction, pulling the yarns paths connected to the un-deformed triangle in the longitudinal region (zone C). In the y-axis triangular zones D, however, some cross-over slippage also took place, meaning that the above mentioned triangles C and D do not go under tension as much as they would in a non-slippage scenario like pin-joint network. This suggests that some neighboring yarns under tension, while fabric shearing, can closely contribute to the onset of local yarn slippage, as also seen often in practical 3D forming cases and maybe viewed as another part defect [10]. It is worth adding that an additional test was performed with smaller sample width so as to remove the full fiber path shown in Figure 5 and see the effect. Results still showed an increase in the x-axis reaction force similar to Figure 7, though with a slightly lower magnitude. Interestingly, in the latter test, the tow slippage was relatively smaller and de-wrinkling rate was slightly higher as the full fiber somewhat path would act as a pin joint arm in the sample.

Finally, in order to characterize the fabric de-wrinkling behavior more distinctively, the de-wrinkling force values from Figure 7 were normalized by the area of the wrinkle at the end of the test, quantified using 3D scanning as explained in section 2.2.3. After removing the effect of area, the theoretically known influence of crossover contact forces [8] at different stages of the shear deformation manifested themselves clearly. The area of wrinkles and normalized de-wrinkling force are plotted against the shear angle of generated wrinkles in Figure 8. The nonlinear trend of the de-wrinkling force would implicitly account for the higher normal forces at cross-over points at higher shear angles. That is, in order to smooth out severe wrinkles, the de-wrinkling force should overcome higher level of established contacts between adjacent years when compared to low-level wrinkles. Also, the area of wrinkles decreased non-linearly during the course of MBBE test (namely, the length of affected area increased while the width decreased rapidly; see also Figure 4c). This can be explained by the fact that as the shear deformation (forming) proceeds, gaps between yarns vanishes and, thus, more severe wrinkles may appear in smaller sizes. It is important to add that in each measured wrinkle state, within the affected area the fiber angles were fairly uniform and the same as that of the corner of the middle region where the fabric was flat (see also Figure 6a). After ~55° shear angle in the middle region, the fiber angle within the wrinkled area stopped increasing (i.e., reaching the lock-up state as shown in Figure 6b), and hence the wrinkle 3 began expanding faster and to a region with a larger length and much lesser width.

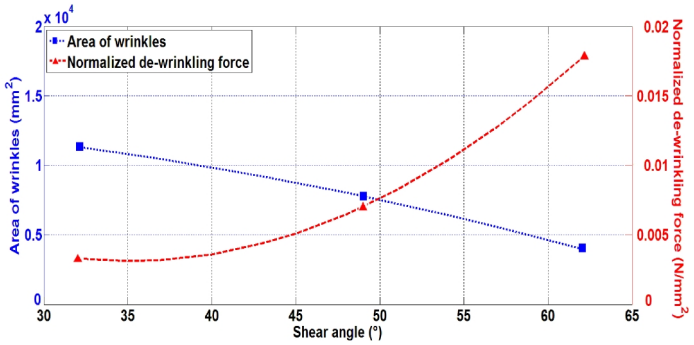

Figure 8. Normalized de-wrinkling force and the area of wrinkles versus shear angle. The area of wrinkles decreases non-linearly as the shear deformation proceeds (also see Figure 6a).

Excerpt from ISBN 978-3-00-053387-7

5. Conclusion

A multi-step biaxial bias extension (MBBE) test procedure was proposed to characterize forming and vanishing of wrinkles of different sizes at shear angles below and above the locking, as both often seen in the composite thermo-forming practice. Employing a 3D scanning technique, the deformation mechanism of the wrinkling/de-wrinkling tests was investigated and the influence of nonlinear contact forces was deemed to be significant when removing wrinkles at high shear angles. Furthermore, contribution of tensioned yarns to slippage was highlighted in the context of 2D characterization of de-wrinkling. Future implementation of the current approach in numerical simulations is expected to enable manufacturers to adjust the optimum blank holder boundary conditions and optimally mitigate wrinkling only in the useful regions of the parts, with no excessive pressure to damage the fibers or cause undesired slippage or jamming of yarns.

Acknowledgments

The authors would like to greatly acknowledge financial support from the Natural Sciences and Engineering Research Council (NSERC) of Canada.

References

[1] W. Lee, M. Um, J. Byun, P. Boisse and J. Cao. Numerical study on thermo-stamping of woven fabric composites based on double-dome stretch forming. *International journal of material forming*, *3*(2):1217-1227, 2010.

[2] P. Boisse, N. Hamila, E. Vidal-Sallé and F. Dumont. Simulation of wrinkling during textile composite reinforcement forming. Influence of tensile, in-plane shear and bending stiffnesses. *Composites Science and Technology*, *71*(5):683-692, 2011.

[3] P. Wang, X. Legrand, P. Boisse, N. Hamila and D. Soulat. Experimental and numerical analyses of manufacturing process of a composite square box part: Comparison between textile reinforcement forming and surface 3D weaving. *Composites Part B: Engineering*, *78*:26-34, 2015.

[4] G. Hivet and A. V. Duong. A contribution to the analysis of the intrinsic shear behavior of fabrics. *Journal of Composite Materials*, *45*(6):695-716, 2011.

[5] H. Lin, J. Wang, A. Long, M. Clifford and P. Harrison. Textile Wrinkling in Composite Forming, 2006.

[6] P. Harrison, F. Abdiwi, Z. Guo, P. Potluri and W. Yu. Characterising the shear–tension coupling and wrinkling behaviour of woven engineering fabrics. *Composites Part A: Applied Science and Manufacturing*, *43*(6):903-914, 2012.

[7] M. Haghi Kashani, A. Rashidi, B. Crawford, Bryn, A.S. Milani. Analysis of a two-way tension-shear coupling in woven fabrics under combined loading tests: Global to local transformation of non-orthogonal normalized forces and displacements. *Composites Part A: Applied Science and Manufacturing, 2016.* (Submitted and under final review)

[8] J. Cao, R. Akkerman, P. Boisse, J. Chen, H. Cheng, E. De Graaf, J. Gorczyca, P. Harrison, G. Hivet and J. Launay. Characterization of mechanical behavior of woven fabrics: experimental methods and benchmark results. *Composites Part A: Applied Science and Manufacturing*, *39*(6), 1037-1053, 2008.

[9] B. Zhu, T. Yu and X. Tao. An experimental study of in-plane large shear deformation of woven fabric composite. *Composites Science and Technology, 67*(2):252-261, 2007.

[10] S. Allaoui, P. Boisse, S. Chatel, N. Hamila, G. Hivet, D. Soulat and E. Vidal-Salle. Experimental and numerical analyses of textile reinforcement forming of a tetrahedral shape. *Composites Part A: Applied Science and Manufacturing*, *42*(6):612-622, 2011.

Excerpt from ISBN 978-3-00-053387-7